Dooris, A., Lakes, R. S., Myers, B. and Stephens, N., "High damping indium-tin alloys", *Mechanics of Time Dependent Materials*, 3, 305-318 (1999).

High damping indium-tin alloys

¤Dooris, A., *Lakes, R. S., ¶Myers, B. and ‡Stephens, N.

¶Anderson Consulting Co.
¤Department of Biomedical Engineering
‡Department of Mechanical Engineering
University of Iowa
Iowa City, IA 52242

*Department of Engineering Physics
Engineering Mechanics Program; Biomedical Engineering Program
Materials Science Program and Rheology Research Center
University of Wisconsin-Madison
147 Engineering Research Building
1500 Engineering Drive, Madison, WI 53706-1687

*Address correspondence to R. Lakes

Key words: alloys, damping, internal friction, aging

ABSTRACT

This research is directed toward the development of materials of high stiffness and high mechanical damping for the purpose of damping vibrations in structures and machinery. To that end, indium-tin alloys are considered. Cast In-Sn exhibits substantial damping for a metal. Quenching substantially improved the damping of indium-tin alloy but the effect gradually disappeared due to aging. Cold work of 1.3 % permanent shear strain had the effect of moderately increasing the damping of indium-tin, and 30 % permanent strain substantially increased the damping of tin.

1. INTRODUCTION

1.1 High damping viscoelastic materials

In viscoelastic materials it is possible to achieve high stiffness and low loss, or high loss and low stiffness, but materials which combine high loss and stiffness are not common, as shown in Fig. 1. Loss or damping is expressed in terms of the phase angle δ between stress and strain for a load history which is sinusoidal in time. The diagonal line in Fig. 1 represents the largest product (0.6 GPa) of stiffness E and linear damping (tan δ) found in common materials.

Passive damping layers of polymers are currently widely used to reduce vibration in machinery such as aircraft and spacecraft. Although polymer layers effective in certain contexts they are not optimal and they suffer the following limitations. For free layer damping, the figure of merit (Wetton, 1979) for the layer material is the product of Young's modulus and mechanical damping: E tan δ. Therefore a combination of high stiffness and high damping is beneficial, but difficult to attain in polymers. For constrained layer damping, it is possible to make use of compliant materials with high tan δ, but only if a substantial amount of *metal* is used in the constraining layer (Cremer and Heckl, 1987). This metal adds weight. Therefore a thinner layer is used in practical damping tapes. Thus the product E tan δ enters the design process indirectly for this method. Again it is difficult to achieve a high value of this product in polymers. Moreover, the α transition associated with peak damping in polymers covers a rather narrow range of temperature. Therefore to achieve damping over a wide temperature range, alternative viscoelastic materials are of interest.

Among metals, lead is commonly thought to be high loss, but its peak damping at about 0.01, is lower than that of tin, cadmium, or indium (Cook and Lakes, 1995a). Lead is also relatively compliant ($G \approx 5.7$ GPa), and it is dense. There are is also a class of manganese copper alloys (called 'Sonoston') which are relatively stiff and provide reasonably high damping and are used for naval ship propellers. Loss tangents as large as 0.014 occur at a stress amplitude of 4000 psi (28 MPa). Mn-Cu alloys are nonlinear, and do not damp well at small stress amplitude (Graesser and Wong, 1991), a significant disadvantage since vibration may occur with a range of amplitude. Mn-Cu alloys exhibit aging in which loss decreases over a period of weeks. It is therefore desirable to create a *linearly viscoelastic* material with a loss tangent of 0.06 or greater, combined with a Young's modulus of 70 GPa or greater, of sufficiently low cost and low density to be practical in applications. A laminate of tungsten and indium-tin was prepared as a proof of concept by Brodt and Lakes, (1995); it exhibited an encouraging combination of stiffness and damping, but tungsten is too dense for most practical use. Cadmium-magnesium alloy has a substantial damping peak (Cook and Lakes 1995b), but it is difficult to prepare. The present study is directed toward modifications of low melting point metals to achieve improved damping. Such metals could be used as a constituent in composites or themselves as a damping layer.

1.2 Viscoelastic mechanisms

There are a variety of causal mechanisms responsible for viscoelastic response. An understanding of these mechanisms can be useful in the development of new viscoelastic materials. Many viscoelastic mechanisms are known (Zener, 1948, Nowick and Berry, 1972). Although the study of relaxation mechanisms has been conducted for some years, the intentional design of materials with high loss based on known mechanisms is relatively recent.

Mechanisms of interest include dislocation drag mechanisms (Schoeck, et al., 1964) in alloys of low melting point. Dislocations are considered to be responsible for "high temperature background" (Schoeck, et al., 1964, Nowick and Berry, 1972) damping at high homologous temperature, defined as the ratio of absolute test temperature to melting point. Metals of low melting point are at high homologous temperature even at room temperature. Some of these metals exhibit substantial damping, $\tan \delta \geq 0.1$.

In composite materials heterogeneous relaxation occurs; provided each phase can be viewed as a continuum, one can predict composite damping and determine optimal composite microstructures (Brodt and Lakes, 1995).

Particulate composites can exhibit thermoelastic damping due to stress induced heat transfer between particles and matrix (Bishop and Kinra, 1994, 1995). For selected regular composite geometries, it is possible to quantitatively calculate the magnitude and characteristic frequency range of thermoelastic damping. The maximum $\tan \delta$ attainable by the thermoelastic mechanism is only about 0.01 but it may help enhance the overall damping in selected frequency ranges.

Available models for dislocation damping in the high homologous temperature regime are insufficient for quantitative prediction of damping or the design of alloys, therefore experiment is required. It is the purpose of this study to experimentally examine several variants of In-Sn alloy which offer increased mechanical damping.

2. EXPERIMENTAL METHODS

2.1 Materials and Fabrication Methods

Eutectic indium-tin alloy and pure tin and indium, all of purity 99.99 % or better, were obtained from Johnson Matthey Alfa.

Fabrication of the alloys was conducted by sealing the metal in a quartz tube and heating under argon in an alloy furnace. The melt was shaken to ensure complete mixing and homogeneity. Various specimens were cast and slowly cooled, cast and rapidly cooled (quenched), and cast and subject to permanent plastic deformation (cold work). Slow cooling was achieved by allowing the specimen to cool within the furnace. Rapid cooling (quenching) was achieved by immersing the specimen tube containing molten metal into a beaker of water. Cold work was achieved by permanently twisting the specimen through an angle sufficient to generate the desired permanent shear strain at the surface. This was done using a calibrated rotation stage, at room temperature. Specimens were 3 to 5 mm in diameter and 20 to 40 mm long.

2.2 Structural Characterization

After viscoelastic testing, the end (~2 mm) of the specimen was cut off using a water-lubricated diamond saw (Buehler Isomet System). This end of the sample was then polished using increasingly fine SiC paper, from 600 through 1000 grit. This was done using a Buehler 8" sanding wheel with constant tap water lubrication. The last SiC polish was performed with ordinary sheet SiC paper (1000 grit), lubricated with general purpose machine oil. Polishing was done slowly, using minimal force against the sanding paper, since the soft metal samples tended to smear rather than abrade. A final polish was obtained using a Buehler Micro polish cloth and a colloidal suspension fluid, followed by water. The specimen was then remounted in the diamond saw and the end was cut again (~2 mm) to obtain a thin disk. Specimens were initially etched with Modified Keller's Formula: 87.5 ml EtOH, 10.0 ml HNO_3, 1.5 ml HCl, 1.0 ml HF. Modified Keller's Formula is typically used in general purpose etching of steels and other structural metals. An alternate etching acid, 1 g picric acid, 90 ml EtOH, 5 ml HCl, was used for some specimens. A subsequent cleaning was performed using an ultrasonic bath with distilled water. Specimens were mounted on SEM stages with conductive double-sided tape.

Scanning electron microscopy (SEM) was performed on a Hitachi S4000 microscope at 5 kV (minimum) excitation voltage. Chamber vacuums ranged from 2 µPa to 4.5 µPa. For most cases the smallest aperture was used with emissions ranging from 5 to 12 µA. Standard procedures were followed for column adjustment and image clarity. Micrographs were taken at various

magnifications from 1000x to 5000x. These were obtained through two different Polaroid systems: the Polaroid Proplan 100 System and 50 ASA Polaroid T-55 film with a 20-25 s development time.

X-Ray analysis was conducted to determine the specimen element constituents. Quantex software running on a Kevex system was used at a 20kV excitation voltage. The rationale for this voltage to excite the La electron in the indium atom. In addition, the specimen working distance was adjusted to 15 mm, the optimal working distance for the detector. Condenser lens aperture was increased, the beam focus increased, and emission increased to boost count rates by increasing the flux on the specimen area in question. Actual settings varied from sample to sample. Data were collected for 60 seconds at a count rate of >10,000 counts per second to ensure statistical significance. After data collection, background noise was subtracted and convolutions performed to delineate peaks, an especially significant factor because of the proximity of In and Sn on the periodic chart. Element search lists were specified and a quasi-numerical analysis of a normalized component composition was obtained. For some specimens the constituents of a particular region was quantified. The electron microscope facilitates such measurement by via either a window or a cross-hair which can be adjusted for size and position in the viewed area.

2.3 Viscoelastic Characterization.

Viscoelastic properties were studied by a method which does not depend on time-temperature superposition (which is used for some polymers but which does not apply to composite materials or to materials in which several relaxation mechanisms are operative). This broadband viscoelastic spectroscopy instrument is capable of determining the dynamic mechanical properties of materials in both torsion and bending over many decades of time and frequency. Torque is applied to the specimen electromagnetically and its deformation is determined by a laser method. Resonances are eliminated from the torque and angle measuring devices by this approach. Resonances remaining in the specimen itself are analyzed by a numerical analysis scheme based on an analytical solution which is applicable to homogeneous cylindrical specimens of any degree of loss. The apparatus is capable of creep, constant load rate, subresonant dynamic, and resonant dynamic experiments in bending and torsion. Measurements in torsion, over an *eleven decade* range of from less than 1 μHz to 100 kHz can be performed, with no appeal to time-temperature superposition. The apparatus (Fig. 2), reported by Brodt, Cook and Lakes (1995) and Lakes and Quackenbush (1996) as a refinement of an earlier device of Chen and Lakes (1989), was further enhanced by addition of magnetic shielding and a Plexiglas® enclosure to exclude air currents.

The observed phase angle is φ, the structural phase angle. It is obtained from the elliptic Lissajous figure (torque vs angular displacement in torsion) by

$$\sin \varphi = \frac{A}{B} \qquad (1)$$

with B as the amplitude of the figure, and A as the width with respect to its center. The quantity of interest is δ, the material phase angle. It is obtained from φ as follows.

$$|G^*| = G' \sqrt{1 + \tan^2 \delta}\,; \qquad (2)$$

$$\tan \delta = \tan \varphi (1 - (\nu/\nu_o)^2) \qquad (3)$$

Here, ν_o is the natural frequency and ν is frequency. G' is the storage shear modulus. This is for a lumped system with end mass much larger than sample mass, but below resonance it is a good approximation to the exact form for a distributed system (Eq. 4); moreover for $\nu << \nu_o$, $\varphi \approx \delta$. The torsional rigidity (ratio of torque M* to angular displacement Φ) of a viscoelastic cylinder of radius R length l, and density ρ with an attached mass of mass moment of inertia I_{at} at one end and fixed at the other end is :

$$\frac{M^*}{\Phi} = [¤\rho\pi R^4][\omega^2 I]\frac{\cot \Omega^*}{\Omega^*} - I_{at}\,\omega^2 \qquad (4)$$

where $\Omega^* = (\rho\omega^2 I^2/KG^*)^{1/2}$, K is a geometrical constant (equal to 1 for a cylindrical specimen with circular cross section). Since damping at high frequency was relatively small, at the resonance angular frequencies ω_o, damping was calculated using the width $\Delta\omega$ at half maximum of the curve of dynamic structural compliance θ/M^* according to $\tan\delta \approx (1/\sqrt{3})\ (\Delta\omega/\omega_o)$.

3. RESULTS AND DISCUSSION

3.1 Effect of quenching

Viscoelastic properties of quickly cooled (quenched) In-Sn are plotted in Fig. 3. Also shown for comparison in Fig. 3 are the data for the slowly cooled In-Sn reported earlier by Lakes and Quackenbush (1996), for which the shear modulus was 7.5 GPa. The slowly cooled In-Sn had aged 192 days at the time of testing while the quenched specimen was tested shortly after casting and again following several increments of aging. The quenched In-Sn showed higher damping but lower stiffness than In-Sn which had been cooled slowly.

The $\tan\delta$ of the In-Sn follows a power law relationship vs. frequency for both the slowly cooled and quenched specimens. The slope for the slowly cooled specimen is -0.28, while the slope for the quenched specimen is initially -0.19. Therefore quenched alloy is less frequency-dependent in its damping than slowly cooled cast alloy. The quenched specimen had a smaller grain size hence more interface area. It is also possible that quenching enhances the density of shorter dislocations. Both structural mechanisms could have the effect of raising the damping of the specimen particularly at the higher frequencies. Overall, in comparison with other metals shown in Fig. 1, the In-Sn alloys have exceptionally high damping properties.

As for aging, observe at 1 Hz and shortly (2.5 hours) after casting, the first quenched specimen had 3 times higher damping than the slowly cooled specimen. After 14 days of aging the quenched specimen was still 1.9 times higher in damping than the slowly cooled specimen. Stiffness, by contrast, increased with aging time. The quenched In-Sn was initially 2.5 times more compliant than the slowly cooled alloy, but after 14 days of aging was only 1.7 times more compliant. By nine months of aging, the damping and stiffness of quenched alloy were within 10% of the values for slowly cooled alloy. Fig. 4 shows the temporal aspects of aging. The effect of aging on the quenched specimen is an increase in stiffness and a decrease in damping. Fitting of a power law in time to the aging curves gave for the stiffness $G \quad t^{0.122}$, and a correlation R = 0.97. Power law fit for the damping $\tan\delta \quad t^{-0.114}$, and a correlation R = 0.95; for a restricted range of eight days, $\tan\delta \quad t^{-0.063}$, and a correlation R = 0.90. Therefore the aging does not appear to be governed by a pure power law.

3.2 Effect of composition

Indium-tin alloys of several compositions were examined. Viscoelastic damping was highest for the eutectic indium-tin alloy as shown in Fig. 5. In the eutectic there is substantial solid solubility, quoted to be 6.5 weight % indium in tin at room temperature (Hansen and Anderko, 1958). Moreover, $\tan\delta$ for eutectic In-Sn exceeds the values observed for pure cast indium. Since this situation does not occur in any known composite (Brodt and Lakes, 1996), the eutectic cannot be simply viewed as a composite. The solid solubility is considered to be linked to the reasons why these materials do not obey the composite theory which would apply to an ideal eutectic. The γ-phase In-Sn, thought to be formed by a peritectic reaction (Hansen and Anderko, 1958) has a hexagonal crystal structure in contrast to the body centered tetragonal structure of Sn. The lower

damping of the tin-rich compositions in comparison with the eutectic or with pure tin suggests a greater constraint of structural features such as dislocations.

3.3 Effect of cold work

Results for cold work in eutectic In-Sn shown in Fig. 6 discloses an increase in tan δ following a small amount of permanent torsional deformation. Fig. 7 shows the effect of permanent deformation on pure tin. Cold work of 30% substantially increased the damping of pure tin. We remark that room temperature is a significant fraction of the melting temperature for these metals, therefore the permanent deformation is not strictly 'cold work' even though the metals were not heated. The increase in damping at high frequency is attributed to the generation of a large number of shorter dislocations during the cold work. The effect of aging for Sn (from 0.95 to 7.1 x 10^5 sec) was less consistent than for In-Sn: for Sn at 0.1 Hz, tan δ $t^{-0.042}$, and R = 0.82; at 1 Hz, tan δ $t^{-0.025}$, and R = 0.73; at 10 Hz, tan δ $t^{+0.023}$, and R = 0.50. The maximum aging for cold worked Sn in this time range was less than that for quenched In-Sn.

3.4 Structure

Photographs of the specimen surfaces are shown in Figures 8 through 12. In all the nitric (Keller's) etched specimens, grain boundaries were completely dissolved, as illustrated in Fig. 8. Keller's etchant caused the mirror finish to become white, possibly as a result of excess dissolution of the surface. Moreover for specimens prepared with Keller's etchant X-ray analysis showed a consistently low percentage of indium. Most likely, the acid was selectively dissolving indium over tin. Despite all these problems, grain boundaries were much more visible using Keller's etchant versus the picric solution in the eutectic and 96% Sn compositions. The picric solution appeared to be less destructive (Fig. 9) but did not clearly reveal boundaries in all cases. X-ray analysis showed particulate inclusions to contain silicon, the main constituent of the SiC abrasive used to polish the specimens. These inclusions are particularly notable in Fig. 9, the picric etched eutectic sample.

As for heterogeneity of composition, what appear to be different phases in the micrographs have only slightly different compositions. Composition changes were on the order of a few percent, therefore the microscopic examination does not reveal the eutectic heterogeneity. Boundary heterogeneity is evident in Fig. 10 and Fig. 11, in which some regions appear spongy (many voids), and other regions, more solid. Typical eutectic layering was not observed. The difficulty in seeing eutectic layering may be attributed to the fact that indium and tin, as neighbors on the periodic chart, exhibit similar contrast in the micrograph. Etching does not bring out visual differences in the constituents of In-Sn alloys.

Grain size observations showed the quenched specimens (Fig. 12) did indeed have decreased grain sizes in comparison with slowly cooled specimens. Compare the quenched specimen center micrograph Fig. 12 to the slowly cooled eutectic, Fig. 9 and 10.

4 CONCLUSIONS

1 Quenching substantially improved the damping of eutectic In-Sn but the effect gradually disappeared due to aging.

2 Eutectic In-Sn had the highest damping among the compositions studied.

3 Cold work of 1.3 % permanent shear strain had the effect of moderately increasing the damping of eutectic In-Sn.

4 Cold work of 30 % substantially increased the damping of pure tin.

ACKNOWLEDGMENTS

Support by the Iowa Space Grant Consortium is gratefully acknowledged.

REFERENCES

Bishop, J. E. and Kinra, V. K., "Elastothermodynamic damping in composite materials", Mechanics of Composite Materials and Structures, 1, 75-93, 1994.
Bishop, J. E. and Kinra, V. K., "Analysis of elastothermodynamic damping in particle-reinforced metal-matrix composites", Metall. and Materials Trans. 26A, 2773-2783, 1995.
Brodt, M., Cook, L. S., and Lakes, R. S., "Apparatus for measuring viscoelastic properties over ten decades: refinements", Review of Scientific Instruments, 66(11), 5292-5297, 1995.
Brodt, M., and Lakes, R. S., "Composite materials which exhibit high stiffness and high viscoelastic damping," Journal of Composite Materials, 29, No. 14, pp. 1823-1833, 1995.
Brodt, M. and Lakes, R. S., "Viscoelastic behaviour in indium alloys: InSn, InBi, InCd and InSnCd", *Journal of Materials Science,* 31, 6577-6581, (1996).
Cook, L. S. and Lakes, R. S., "Damping at high homologous temperature in pure Cd, In, Pb, and Sn", Scripta Metall et Mater., 32, 773-777, 1995a.
Cook, L. S. and Lakes, R. S., "Viscoelastic spectra of $Cd_{0.67}Mg_{0.33}$ in torsion and bending", Metallurgical and Materials Transactions, 26A, 2037-2039, 1995b.
Cremer, L. and Heckl, M., *Structure borne sound*, 2nd Ed., Springer Verlag, Berlin, 1987.
Chen, C. P. and Lakes, R. S., "Apparatus for determining the properties of materials over ten decades of frequency and time", Journal of Rheology, 33(8): 1231-1249, 1989a.
Graesser, E. J. and Wong, C., "Analysis of strain dependent damping in materials via modeling of material point hysteresis", DTRC-SME-91/34, July 1991; David Taylor Research Center, Bethesda, MD.
Hansen M. and Anderko, K. *Constitution of Binary Alloys*, McGraw-Hill, New York (1958).
Kinra, V. K., Wren, G. G., Rawal, S., and Misra, M., "On the influence of ply-angle on damping and modulus of elasticity of a metal-matrix composite", Metall. Trans. 22A, 641-651, 1991.
Lakes, R. S., "Materials with structural hierarchy", *Nature*, 361, 511-515, 1993.
Lakes, R. S. and Quackenbush, J., "Viscoelastic behaviour in indium tin alloys over a wide range of frequency and time", Philosophical Magazine Letters, 74, 227-232, 1996.
Lakes, R. S., *Viscoelastic solids*, CRC Press, Boca Raton, FL, (1999).
Nowick, A. S. and Berry, B. S., *Anelastic relaxation in crystalline solids*, Academic, NY, 1972.
Schoeck, G., Bisogni, E., and Shyne, J., "The activation energy of high temperature internal friction," *Acta Metallurgica*, **12**, 1466-1468 (1964).
Wetton, R. E., "Design of elastomers for damping applications", in *Elastomers: criteria for engineering design*, ed. Hepburn, C., Reynolds, R. J. W., Applied Science Publishers, LTD, London, 1979.
Zener, C., *Elasticity and anelasticity of metals,* University of Chicago Press, 1948.

Figure Captions

Fig. 1 Stiffness loss map, showing experimental results for Young's modulus E and mechanical damping tan δ for various common materials at selected frequencies, after Lakes (1999). The diagonal line represents $|E^*| \tan \delta$ = constant, and most common materials are represented by points to the left of that line. The region in the upper right is favorable for vibration damping applications.

Fig. 2 Broadband viscoelastic spectroscopy apparatus.

Fig. 3. Comparison of slowly cooled (after Lakes and Quackenbush, 1996) vs. quenched eutectic In-Sn including early aging of quenched In-Sn. (Room temperature, 296K. No appeal made to time-temperature superposition.)

Fig. 5 Effect of composition of cast In-Sn alloy. Datum for γ In-Sn after Lakes and Quackenbush (1996). Dash line is solely intended as a guide for the eye.

Fig. 6 Effect of cold work (permanent shear strain) is to moderately increase the damping of cast In-Sn alloy.

Fig. 7 Effect of cold work (permanent shear strain) in pure tin. A substantial increase in damping is possible. Effects exhibit aging. ♦, age, $9.5 \cdot 10^4$ sec; smaller symbols, 2.6, 7.1, $8.8 \cdot 10^5$ sec. +, age, $6.1 \cdot 10^4$ sec; smaller symbols, $1.5 \cdot 10^5$ sec.
Fig. 8 Eutectic In-Sn nitric etched.
Fig. 9 Eutectic In-Sn picric etched.
Fig. 10 65% In-Sn, picric etched.
Fig. 11 Gamma In-Sn, picric etched.
Fig. 12 Quenched eutectic In-Sn.

Figures

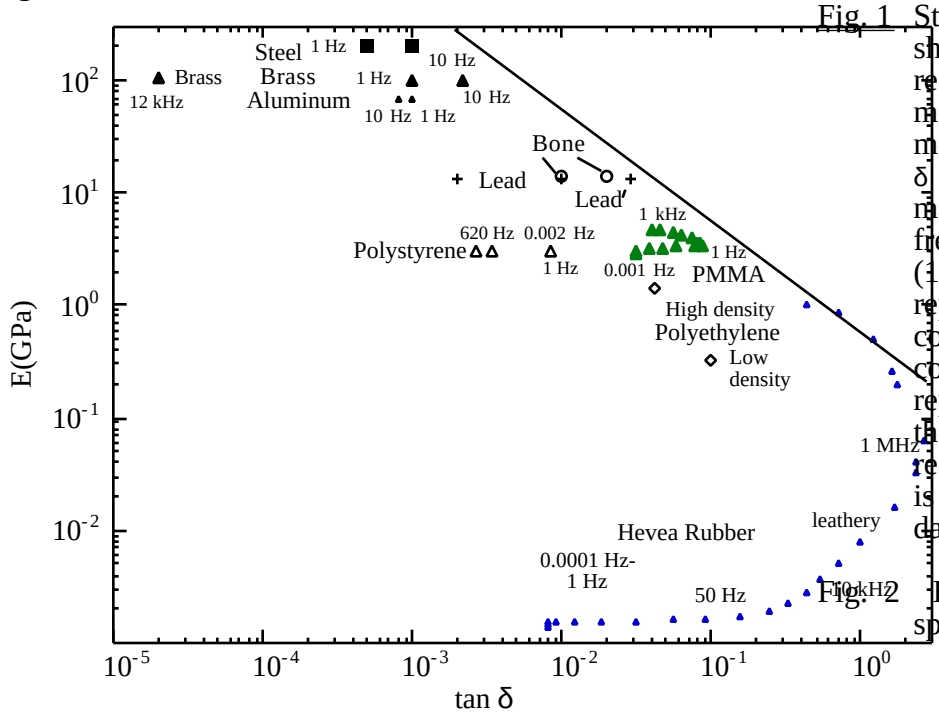

Fig. 1 Stiffness loss map, showing experimental results for Young's modulus E and mechanical damping tan δ for various common materials at selected frequencies, after Lakes (1999). The diagonal line represents |E*| tan δ = constant, and most common materials are represented by points to the left of that line. The region in the upper right is favorable for vibration damping applications.

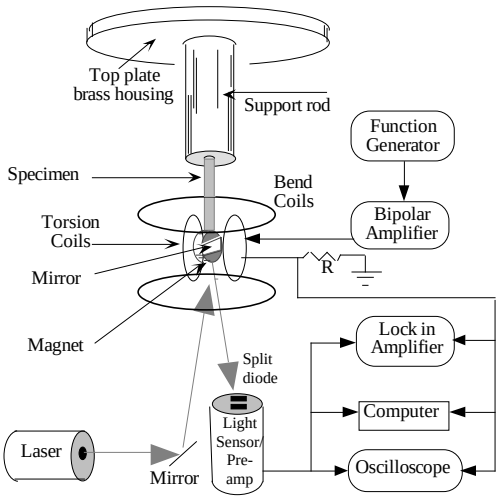

Fig. 2 Broadband viscoelastic spectroscopy apparatus.

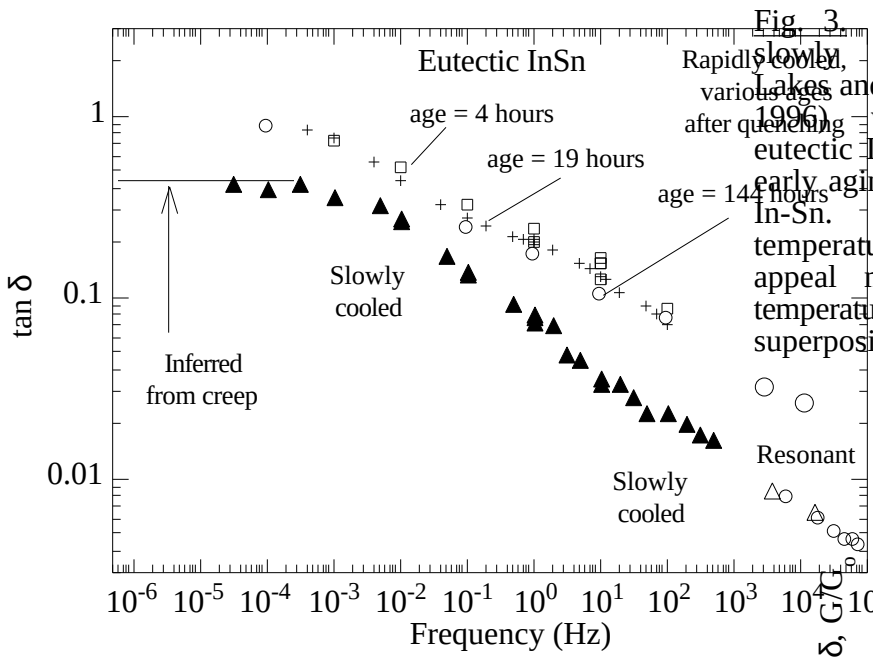

Fig. 3. Comparison of slowly cooled (after Lakes and Quackenbush, 1996) vs. quenched eutectic In-Sn including early aging of quenched In-Sn. (Room temperature, 296K. No appeal made to time-temperature superposition.)

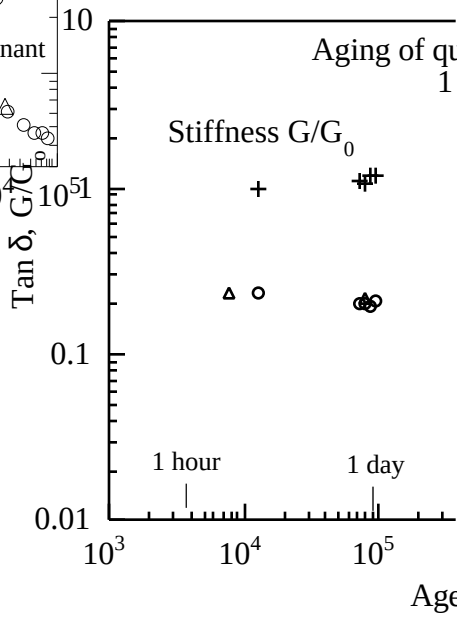

Fig. 4 Aging of quenched indium-tin alloy.

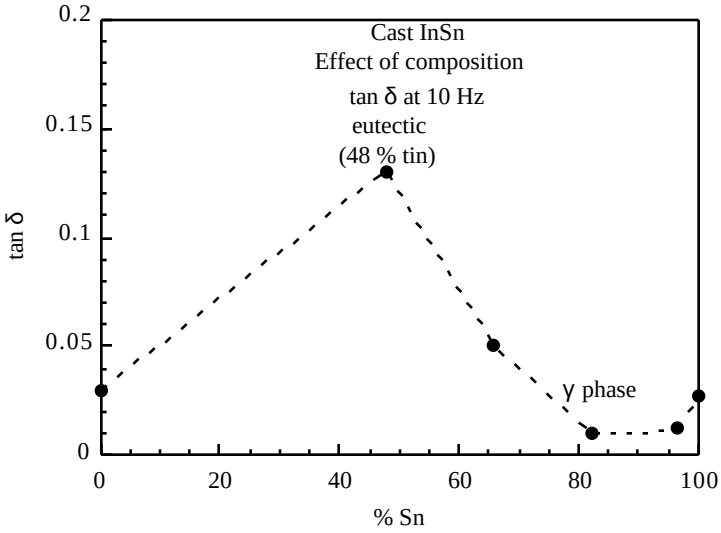

Fig. 5 Effect of composition of cast In-Sn alloy. Datum for γ In-Sn after Lakes and Quackenbush (1996). Dash line is solely intended as a guide for the eye.

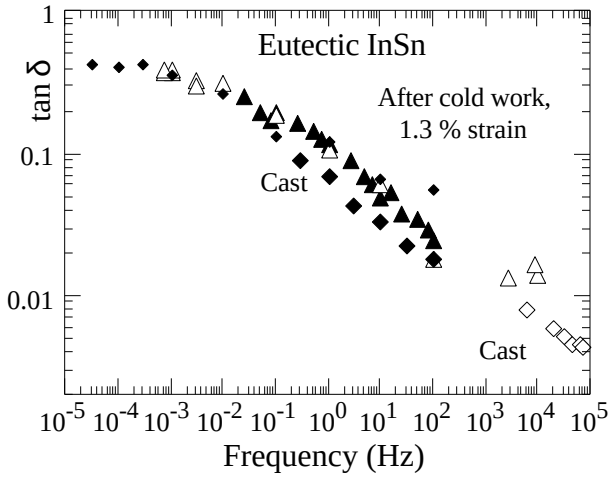

Fig. 6 Effect of cold work (permanent shear strain) is to moderately increase the damping of indium-tin alloy.

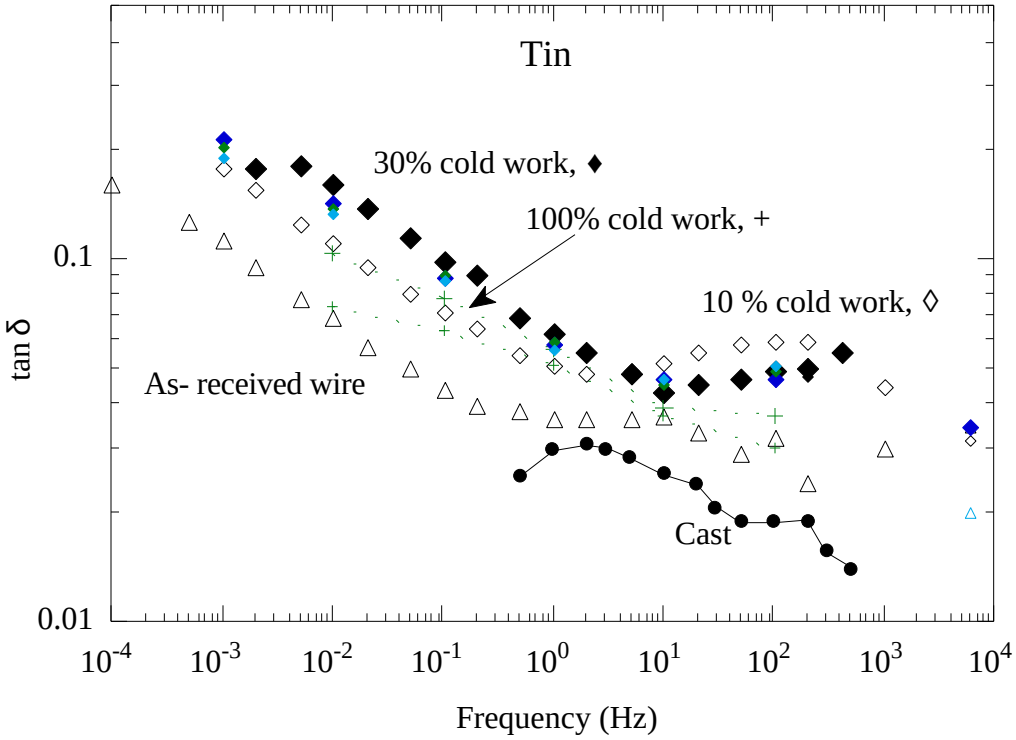

Fig. 7 Effect of cold work (permanent shear strain) in pure tin. A substantial increase in damping is possible. Effects exhibit aging. ♦ , age, $9.5 \cdot 10^4$ sec; smaller symbols, 2.6, 7.1, $8.8 \cdot 10^5$ sec. +, age, $6.1 \cdot 10^4$ sec; smaller symbols, $1.5 \cdot 10^5$ sec.

Fig. 8 Eutectic In-Sn nitric etched.

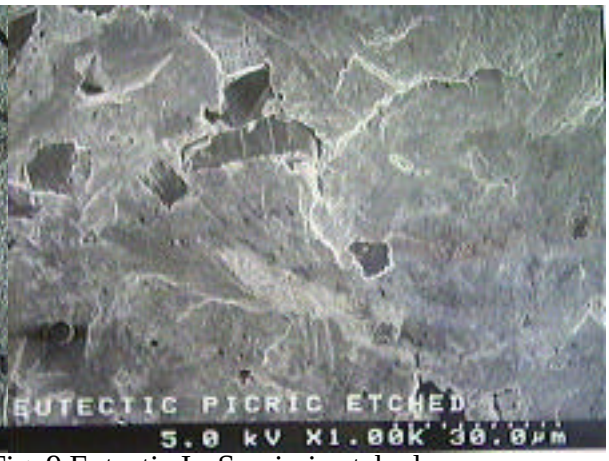

Fig. 9 Eutectic In-Sn picric etched.

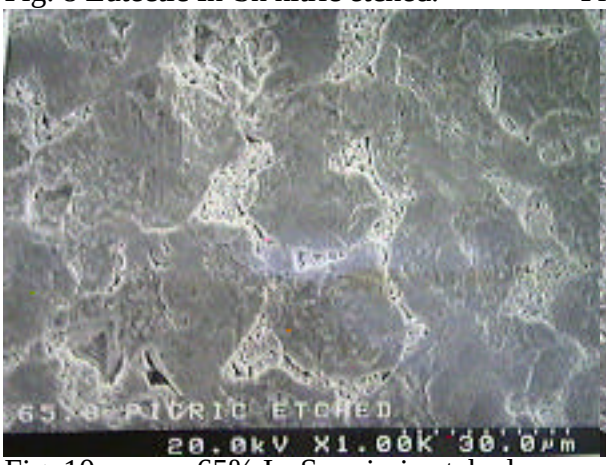

Fig. 10 65% In-Sn, picric etched.

Fig. 11. Gamma In-Sn, picric etched.

Fig. 12 Quenched eutectic In-Sn .